

Sound Speed Resonance in the Gravitational Wave Background as a probe for non-standard early universe cosmologies

Igor de O. C. Pedreira,^{a,b,c} Amara Ilyas,^{a,b} Ziwei Wang,^{d,e} Leila L. Graef,^c Yi-Fu Cai^{a,b}

^aDepartment of Astronomy, School of Physical Sciences, University of Science and Technology of China, Hefei, Anhui 230026, China

^bCAS Key Laboratory for Researches in Galaxies and Cosmology, School of Astronomy and Space Science, University of Science and Technology of China, Hefei, Anhui 230026, China

^cInstituto de Física, Universidade Federal Fluminense, 24210-346 Niteroi, RJ, Brazil

^dDepartment of Strategic and Advanced Interdisciplinary Research, Pengcheng Laboratory, Shenzhen, Guangdong 518066, China

^eKey Laboratory of Dark Matter and Space Astronomy, Purple Mountain Observatory, Chinese Academy of Sciences, Nanjing 210033, China

E-mail: igorpedreira@id.uff.br, aarks@ustc.edu.cn, wangzw@pcl.ac.cn, leilagraef@id.uff.br, yifucai@ustc.edu.cn

Abstract. Gravitational waves constitute a powerful probe of the underlying theory of gravity. In extensions of general relativity, additional degrees of freedom, such as scalar fields in the gravitational sector, can modify their propagation through changes in the effective friction term and propagation speed. These modifications may potentially induce resonant phenomena leading to distinctive signatures in the gravitational wave spectrum. One important aspect to be investigated is whether the resonances can be strong enough to enhance the underlying background of primordial tensor modes to levels detectable by upcoming gravitational wave detectors, such as LISA or the Einstein telescope. The characteristic peaks in the SBGW spectrum depend on the parameters of the resonant model as well as on the parameters of the primordial tensor spectrum, such as r and n_t . Thus these resonance effects open a powerful pathway to explore physics of the very early Universe by amplifying otherwise feeble signals to experimentally detectable levels. Here we analyze how the signals of the primordial Universe can resonate in these scenarios, bringing the early universe physics into the realm of experimental access.

Contents

1	Introduction	1
2	The Spectrum of the Gravitational Waves	4
2.1	Primordial Gravitational Waves	4
2.1.1	Solution for the perturbations modes	5
2.2	Astrophysical Foreground	6
2.3	Big Bang Nucleosynthesis Bound	7
3	Parametric Resonance in DHOST	8
3.1	ULDM scenario	8
3.1.1	Key Parameters	10
4	Results and Discussion	11
4.1	The spectrum of SGWB in the presence of resonance: The role of each parameter	13
4.2	Probing the primordial spectrum parameters with resonance	14
5	Conclusion	16

1 Introduction

Research on Gravitational Waves (GW) have grown in the past decade, since the first detection from astrophysical sources by LIGO [1]. Since then, the community has intensified its efforts to detect gravitational wave signals across all frequencies. Later in 2023 strong evidence on the presence of a stochastic signal in the Pulsar Timing Arrays data was reported by NANOGrav [2], and later, similar levels of evidence were reported by several other PTA collaborations [3–5]. Besides astrophysical sources, cosmological phenomena can also generate a stochastic background of gravitational waves (SGWB). Among the cosmological sources [6], we can mention the quantum fluctuations generated in the very early universe, which are stretched out from the Hubble radius, and later, when re-entering the Hubble horizon, behave like relic gravitational waves, forming a stochastic background.

Compared to the astrophysical signals, cosmological sources can predict different shapes for the SGWB power spectrum, which can be probed across all frequency ranges. The power spectrum of the primordial GW can be parametrized by the tensor-to-scalar ratio r , constrained by the PLANCK collaboration [7, 8], and the tensor spectral index n_t . There exists a wide variety of models in the literature predicting either a blue-tilted spectrum ($n_t > 0$) or a red-tilted spectrum ($n_t < 0$). However, no direct observational constraint on the tensor spectral index is currently available [9–11].

Models predicting a blue tilt are of particular interest, since they enhance the gravitational wave amplitude at higher frequencies, potentially bringing the signal within the sensitivity range of current or future GW detectors. Additional mechanisms can also predict spectra with a signal that grows with the frequency across different frequency bands. These include, for instance: non-canonical inflationary models [12–21], non-instantaneous reheating [10, 22, 23], natural inflation coupled to gauge fields [24–28], bounce models [29–36], cosmological first-order transitions [37–41], particle production [42–44], axion couplings [45–50] departures from GR and modified gravity theories [51–62].

The GW detections nowadays happen mainly in earth-based interferometers, such as the LIGO-VIRGO-KAGRA collaboration [63–65] in the $10^0 - 10^4$ Hz frequency range. A future earth-based detector that will considerably improve the current detector’s sensitivity in the high frequency range will be the Einstein Telescope [66–68] an underground interferometer operating in the $10^{-3} - 10$ Hz frequency range planned for later in the 2020’s. In a lower frequency range $10^{-5} - 10^{-1}$ Hz, the LISA space interferometer is planned to be launched in the next decade [69–72]. In even lower frequencies, Pulsar Timing Arrays (PTA) may, in the near future, allow to probe the SGWB signal in the nanohertz frequency band [2, 5, 6, 73–80]. Probing a similar frequency range, the Square Kilometer Array (SKA) [81], shall soon start operating increasing considerably the sensitivity in this band.

So far the Planck satellite has imposed an upper limit on the tensor-to-scalar ratio to be $r < 0.035$ [82]¹. Other CMB experiments, such as SPT-3G [85–88] and especially the LITEBIRD satellite [89–91], which is being planned to search for these B-modes, intend to measure the tensor-to-scalar ratio up to a level of 10^{-3} (for a review, check the reference [92]). In the literature, there have been various models to study a decrease in the value of r [14, 93–98]. In addition to CMB constraints, an important constraint on the SBGW spectrum comes from the Big Bang Nucleosynthesis (BBN) bound on the relativistic degrees of freedom on the primordial universe, which puts an upper limit on the amplitude of the GW spectrum across a long range of frequencies [9, 99–101].

The search for SBGW can be of paramount importance not only to probe the physics of inflation but also as a test for possible departures of general relativity (GR) [102–104]. Modified gravity theories arises as a interesting alternatives to GR, offering possible explanations for several outstanding problems in cosmology. These include the origin of the current accelerated expansion [105–112], explain the evolution of the primordial universe [113–116], or even the behavior and nature of dark matter [117–120]. In many cases, such theories are constructed by introducing additional degrees of freedom, most commonly a scalar field, alongside the usual tensor modes of GR. These frameworks are generally referred to in the literature as scalar–tensor theories [106].

The dynamics of scalar fields in modified gravity theories under certain conditions may cause an amplification of the gravitational wave spectrum. Time-oscillations of such fields at the bottom of their potential may lead to an effect called parametric resonance, which results in a exponential enhancement of GW power, leaving significant imprints in different frequencies of the GW spectrum [121–123]. This effect is also called sound speed resonance (SSR), because those resonances can cause changes in the propagation speed of the sound waves due to the scalar field, and has previously been studied in the literature [124–130].

In recent years, the possibility of the existence of ultra light scalar fields non minimally coupled to gravity started to get more attention in community, because such a field can be considered as a possible candidate for constituting a class of dark matter named ultra light dark matter (ULDM). These kind of particles can arise from axion models[131–134], dark photons [135–138] or light particles generated in string theory models [139–145]. Those particles are proposed as a way to address the behavior of dark matter in small scales, maintaining the large scale behavior intact. Such particles can exhibit a wave-like nature, thanks to its low mass $m \sim 10^{-22} - 10^0$ eV. Such wave-like nature can help resisting the collapse of dark matter halos at galaxy scales and suppress the formation of small mass halos [118, 146–153].

¹Tighter upper limits on r can be obtained by combining Planck data with other cosmological probes, as shown, for instance, in Ref. [83, 84]. These constraints are of the same order as the Planck-only bounds, which we adopt in the present analysis.

ULDM provides a well-motivated example of a coherently oscillating scalar field. When such a scalar is non-minimally coupled to gravity, its oscillations can induce periodic time dependence in the propagation of gravitational waves, leading to the parametric resonance phenomena previously mentioned. In this paper we will consider an ULDM field in the context of scalar tensor theories with higher order derivatives, given by quadratic Degenerate Higher Order Scalar Tensor (DHOST) Theories [106, 154–157], which avoid the presence of the so called Ostrogradski instability that plagues general scalar tensor formulations [158, 159]. In this class of theories, the amplification of the GW power spectrum can happen due to a change in the propagation speed of the gravitational waves, in the friction term or due to modifications on the background evolution which alters the Friedmann Equation [160–162]. We will reduce the functional freedom of DHOST theories by the use of disformal transformations to work in the frame where tensor modes propagate as in GR [163–165]. In this frame, parametric resonances arising from the oscillations in the GW propagation speed can be associated to oscillations in the scale factor of the GW frame, which help us find potential cancellation effects. In order to simplify our calculations, we will consider an Effective Field Theory (EFT) approach for DHOST and require that the modifications are below the cut-off scale of the EFT [162, 166]. We consider the DHOST scenario in which the stochastic gravitational wave background evolves through a standard radiation-dominated universe, producing a smooth baseline spectrum as predicted by GR [162]. We will consider that certain modes experience resonant amplification due to time-dependent modifications in the gravitational-wave propagation on this smooth baseline. Most other modes continue to follow the standard evolution, resulting in narrow, localized bands that stand out on the background spectrum.

Our interest in this work is to test whether the resonance bands can be used as a way to probe a non-standard background evolution of the early universe. In principle, the resonance effect can happen in different periods of the evolution of the universe, but we focus on it happening during radiation domination era. We will explore how the amplitude of these resonant bands is affected by the underlying primordial tensor spectrum. We assume the primordial tensor spectrum to follow the standard parametrization, without supposing that modified gravity theory affects the generation of the tensor modes. We will remain agnostic on the underlying early universe scenario, whose spectrum we simply parametrize by different combinations of the tensor-to-scalar ratio r and the tilt of the tensor spectrum n_t . This approach allows us to explore a broad range of scenarios, with particular emphasis on blue-tilted primordial spectra, as these can enhance the gravitational-wave amplitude at frequencies within the sensitivity band of LISA. Specifically, we are going to analyze how the SSR effect caused by the dynamics of ULDM oscillations in a quadratic DHOST theory can affect the detection prospects of the SGWB in different early universe scenarios. While the quantitative analysis here will be carried out for ULDM scalar field within the framework of DHOST scalar tensor theories, we argue that the underlying mechanism is more general. Despite the quantitative results remains model-dependent, any consistent modified gravity theory in which an oscillating scalar field directly modulates the GW propagation coefficients can, in principle, exhibit similar resonant effects. DHOST theories provide a controlled and observationally viable setting, free of instabilities and compatible with gravitational-wave constraints, but the qualitative conclusions extend to broader classes of scalar tensor theories.

This paper is organized as follows: In section 2, we present the derivation of the expression for the GW spectral energy density and we comment about the astrophysics foregrounds and the BBN limits. In section 3, we describe the ULDM scenario that predicts the paramet-

ric resonance effect. In Section 4, we present our results and demonstrate how the resonance reshapes the region of parameter space accessible to LISA in the r - n_T plane. Finally, we give our final remarks in section 5.

2 The Spectrum of the Gravitational Waves

In this section, we review the derivation of the stochastic gravitational wave background spectrum arising from tensor perturbations of the Friedmann-Lemaitre-Robertson-Walker (FLRW) metric.

2.1 Primordial Gravitational Waves

If we consider small perturbations ($|h_{ij}| \ll 1$) over an isotropic and homogeneous FLRW metric in the transverse traceless gauge ($\partial_i h_{ij} = h_{ii} = 0$), at first order, one can write the line element as [167]:

$$ds^2 = a^2(\eta) [-d\eta^2 + (\delta_{ij} + h_{ij})dx^i dx^j] . \quad (2.1)$$

By using this metric in the Einstein equation, we obtain a second order differential equation for the evolution of the perturbation h_{ij} . In Fourier space, we can write for both polarization modes [10]:

$$h_k''^{\mu\lambda} + 2\frac{a'}{a}h_k'^{\mu\lambda} + k^2 h_k^{\mu\lambda} = 0 , \quad (2.2)$$

where the prime $'$ denotes derivative with respect to conformal time $d/d\eta$. With the solution of this equation, we can write down the gravitational wave spectrum as:

$$\Omega_{GW}(k, \eta) = \frac{1}{\rho_c(\tau_0)} \frac{\partial \rho_{GW}(k, \tau)}{\partial \ln k} . \quad (2.3)$$

where $\rho_c = H_0^2/8\pi G$ is the critical density of the universe today and ρ_{GW} is related to the perturbation coefficient as [168]:

$$\rho_{GW}(k, \eta) = \frac{\langle h'_{ab} h'^{ab} \rangle}{32\pi a^2 G} \quad (2.4)$$

We can rewrite the numerator on the right side of eq. (2.4) in terms of the power spectrum, defined as: $\mathcal{P}_T(\eta, k) = 2k^3/2\pi^2 \langle h_{ij} h^{ij} \rangle$. We can also rewrite the primordial power spectrum in terms of the transfer function $\mathcal{T}(\eta, k)$ as:

$$\mathcal{P}_T(\eta, k) \equiv \mathcal{P}^{prim}(k) \times [\mathcal{T}(\eta, k)]^2 . \quad (2.5)$$

$\mathcal{P}^{prim}(k)$ is related to the modes that left the horizon during the inflation and can be parametrized as a power law around the CMB pivot scale, $k_* = 0.05 Mpc^{-1}$ [28]:

$$\mathcal{P}^{prim}(k) \equiv A_T \left(\frac{k}{k_*} \right)^{n_t} , \quad (2.6)$$

where A_T is the amplitude of the primordial tensor perturbations, which can be written in terms of the amplitude of scalar perturbations A_S and the tensor-to-scalar ratio r : $A_t = r \times A_S$. The transfer function describes the subsequent time evolution of the perturbation

modes, and is defined as $\mathcal{T}(\eta, k) \equiv \frac{h_k(\eta)}{h_k^{prim}}$. By using all the previous equations, we can write the expression for the GW power spectrum as:

$$\Omega_{GW}(k, \eta) = \frac{1}{12a^2(\eta)H^2(\eta)} \left[\frac{d}{d\eta} \mathcal{P}_T(\eta, k) \right]^2 = \frac{\mathcal{P}^{prim}(k)}{12a^2(\eta)H^2(\eta)} [\mathcal{T}'(\eta, k)]^2. \quad (2.7)$$

Although primordial power spectrum of gravitational wave generated by slow roll inflation has to obey the consistency relation [121, 169], in which the tensor-to-scalar ratio r and the spectral index n_t are related via: $n_t = -\frac{r}{8}$, indicating a slightly red spectrum, there are early universe scenarios predicting blue tilted spectrum of gravitational wave. For example:

- Fields satisfying the violation of the Null Energy Condition (NEC) during inflation, such as G-inflation [170], break the consistency relation, which can produce a blue tilted tensor perturbation.
- If the universe underwent a distinct kinetic or geometric phase prior to the standard inflationary expansion, the initial vacuum state of the perturbations can be altered into a non-Bunch-Davies state (often parameterized as α -vacua).² The mode mixing—described by Bogoliubov transformations between the standard Bunch-Davies vacuum and the actual state—modifies the amplitude and scale dependence of the power spectra. Depending on the precise Bogoliubov coefficients generated by the pre-inflationary transition, this can introduce a scale-dependent modifications that tilts the tensor spectrum blue [174].

The scenarios mentioned above predict $n_t > 0$ and break the consistency relation between n_t and r , respectively. In this work, rather than discuss early universe scenarios in detail, we parameterize the primordial tensor perturbations with free parameters r and n_t not supposing any consistency relation and study the enhancement of gravitational waves through parametric resonance phenomenologically.

2.1.1 Solution for the perturbations modes

The evolution of the modes h_k is very complicated and cannot be solved analytically for a random expansion history [168, 175]. But for constant equation of state ω , it has been obtained before in the literature for different scenarios [176].

The gravitational waves we measure today are supposed to be originated by quantum fluctuations in the primordial universe. As the universe undergoes accelerated expansion during inflation, those modes are stretched to super-horizon scales ($k < aH$) and freeze, which leads to $h_k^{prim} \propto \text{Const.}$ [177]. When they re-enter the horizon they evolve classically, according to $h_k(\tau) = h_k^{prim} \times \mathcal{T}(\eta, k)$.

When the modes are deep inside the horizon, as the case that will be considered in this paper, we can approximate the solution for the evolution of the modes considering the WKB approximation [177, 178]. Considering that, the modes can be approximate as:

$$h_k(\eta) \propto \frac{1}{a(\eta)} e^{\pm ik\eta}. \quad (2.8)$$

²Historically, such modified initial states were sometimes invoked to model effective trans-Planckian physics [171]. However, the Trans-Planckian Censorship Conjecture (TCC) posits that in a consistent quantum theory of gravity, modes that originate at sub-Planckian scales are strictly forbidden from exiting the Hubble radius and becoming macroscopic [172, 173].

With it, it's possible to rewrite the transfer function as the following expression:

$$\mathcal{T}(k\eta) = \frac{a(\eta_{hc})}{a(\eta)} e^{\pm ik\eta}. \quad (2.9)$$

To construct the spectrum, we will need the derivative of the transfer function squared. By considering eq. (2.9), and using the fact that $k = a_{hc}H_{hc}$ during the reentry, we can rewrite [177]:

$$[\mathcal{T}'(k\eta)]^2 \approx \frac{k^2}{2} \left(\frac{a(\eta_{hc})}{a(\eta)} \right)^2 = \frac{a^4(\eta_{hc})H^2(\eta_{hc})}{2a^2(\eta)}. \quad (2.10)$$

Applying eq. (2.10) to eq. (2.7), we obtain the following expression for the spectrum:

$$\Omega_{GW}(k, \eta) = \frac{\mathcal{P}^{prim}(k)}{24} \frac{a^4(\eta_{hc})H^2(\eta_{hc})}{a^4(\eta)H^2(\eta)}. \quad (2.11)$$

We can rewrite this expression by considering that in the horizon crossing $H^2 = \Omega_\omega H_0^2 a^{-3(1+\omega)}$, where Ω_ω is the density parameter of the dominant component of given epoch, and $k = a_{hc}H_{hc}$. Therefore,

$$k \propto a_{hc}^{-\frac{1+3\omega}{2}}. \quad (2.12)$$

Using this expression we obtain for the spectrum today,

$$\Omega_{GW}(k, \eta_0) = \frac{\mathcal{P}^{prim}(k)\Omega_\omega}{24a_0^4H_0^2} k^{2\left(\frac{\omega-1/3}{\omega+1/3}\right)}. \quad (2.13)$$

By using the parametrization given by Eq. (2.6) and using the relation between wave-number and frequency:

$$f = \frac{1}{2\pi} \frac{k}{a_0}, \quad (2.14)$$

we can obtain the final expression for the spectrum of the modes that re-enter the horizon during radiation-dominated ($\omega = 1/3$) era as³ [179, 180]:

$$\Omega_{GW}(f, \eta) = \frac{\Omega_{rad}}{24} r_{AS} \left(\frac{f}{f_\star} \right)^{n_t}. \quad (2.15)$$

2.2 Astrophysical Foreground

A stochastic signal generated by the population of binary systems scattered around our galaxy could be measured by the current and next generation GW detectors. This signal usually comes from "unresolved" sources, that do not come from a single event, but composes a stochastic background [181]. If that signal is not strong enough, it could go undetected or could be indistinguishable from noise. It is crucial to understand the expected astrophysical signal across the frequencies bands probed by the detectors.

The main sources of astrophysical foreground in different frequency ranges are: the unresolved populations of Galactic and Extragalactic White Dwarfs binaries (GWD and EGWD, respectively); the unresolved stellar mass binaries of Black Holes (BBH), Neutron Stars (BNS) and Black Hole- Neutron Star binary (BH-NS). It is possible to make approximate analytical fits for the astrophysical foreground's contributions [182].

³By eq. (2.14), the CMB pivot scale k_\star corresponds to a frequency of $f_\star = 7.5 \cdot 10^{-15}$ Hz.

Inside the LISA detection band, those three astrophysical systems give the major contribution to the astrophysical foreground signal. Usually, those contributions are represented in terms of the spectral density $S_h(f)$ [175, 183]. By writing the contributions in terms of the spectral density, the comparison with the signal-to-noise ratio becomes more transparent. The spectral density is related with the GW spectrum through the equation[184],

$$\Omega_{GW}(f) = \frac{4\pi^2}{3H_0^2} f^3 S_h(f). \quad (2.16)$$

The expression for the spectral density of different astrophysical sources can be found, for instance in Ref. [182]. By substituting those expressions in equation (2.19), we obtain the equation approximating the SGWB spectrum for each astrophysical foreground:

$$\Omega_{\text{fg}}^{\text{gal}}(f) = \frac{2\pi^2}{3H_0^2} A f^{2/3} e^{-f^\alpha + \beta f \sin(\kappa f)} [1 + \tanh(\gamma(f_k - f))], \quad (2.17)$$

$$\Omega_{\text{fg}}^{\text{exgal}}(f) = \frac{2\pi^2}{3H_0^2} \times 4.2 \times 10^{-47} \left(\frac{f}{1 \text{ Hz}}\right)^{-4/3} \exp\left(-2\left(\frac{f}{5 \times 10^{-2} \text{ Hz}}\right)^2\right), \quad (2.18)$$

$$\Omega_{\text{fg}}^{\text{BBH+BNS}}(f) = \Omega_{\text{ref}} \left(\frac{f}{f_{\text{ref}}}\right)^{2/3}, \quad (2.19)$$

Those previous equation were obtained by using the parametrization of Ref. [185, 186] for the galactic WD in Eq. (2.17), where the values (present in table 1) were taken from Ref. [186]; the analytical approximation given in Ref. [187] for the extragalactic WD for Eq. (2.18); an approximate power law for the contribution of the BBH and BNS system, with parameters $\Omega_{\text{ref}} = 9.0 \times 10^{-10}$ at a frequency $f_{\text{ref}} = 25\text{Hz}$, following Ref. [188]. In figure 1, we can see the astrophysical contributions for the stochastic GW spectrum that can contribute to a detectable a signal inside the LISA frequency band.

A	9×10^{-45}
α	0.138
β	-221
κ	521
γ	1680
f_k	0.00113

Table 1: Parameters used for the galactic WD spectrum in Eq. (2.17), according with the 4yr observation time. Values are taken from Ref. [186].

2.3 Big Bang Nucleosynthesis Bound

In principle, the GW can be generated with any amplitude, depending on the physics that creates those modes and how they evolve, as we can see from Eq. (2.15). Although, there are a few limits on the spectrum arising from the observations. First, we have a detection upper bound from the absence of a cosmological signal in higher frequencies from the LIGO/VIRGO/KAGRA detectors of the order $\Omega_{\text{GW}} \leq 6.0 \times 10^{-8}$ in the reference frequency $f_{LV} = 25\text{Hz}$ [189]. On the other hand, in the lowest frequencies we have constraints imposed by the CMB experiments.

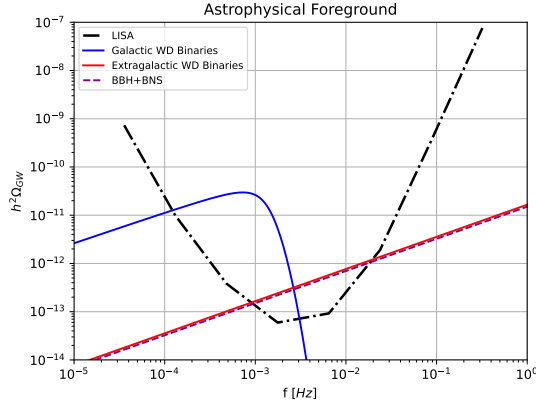


Figure 1: SGWB spectrum for the astrophysical foreground. We shown the unresolved Galactic WD in blue, the unresolved Extragalactic WD in red and the sum of the BBH and BNS in magenta. In Black, we show the LISA’s sensitivity curve.

In addition, the big bang nucleosynthesis implies in a constraint to a broad frequency range of the spectrum. Primordial gravitational waves contributes to the total energy density of the extra relativistic species during the early universe, which changes the expansion rate and affects the abundance of the light elements. In order to not violate the BBN bound, the total energy density of the gravitational waves should obey [189]:

$$\int_{f_{BBN}}^{f_{end}} d(\ln f) \Omega_{GW}(f) h^2 \leq 5.6 \cdot 10^{-6} \left(N_{eff}^{(Upper)} - 3.046 \right), \quad (2.20)$$

where $N_{eff}^{(Upper)}$ is the upper bound on the effective number of relativistic degrees of freedom, taken to be $\Delta N_{eff} = N_{eff}^{(Upper)} - 3.046 \sim 0.300$ [190], the lower limit in the integral is taken to be frequency corresponding to the mode entering the horizon at the time of BBN $f_{BBN} = 10^{-10}$ Hz and $f_{end} = 10^7$ Hz is set to be the scale on the end of inflation, which correspond to a temperature around 10^{15} GeV [100, 189].

3 Parametric Resonance in DHOST

In the previous section, we discussed the spectrum of the SGWB from cosmological origin and the astrophysical foreground expected within the LISA detection band. However, it remains to be studied how parametric resonance affects this background. In this section, we describe the ULDM formalism and its influence on the gravitational wave background.

3.1 ULDM scenario

Let us consider a ULDM setup where a parametric resonance of the Gravitational Waves occurs due to modifications in the background during the radiation dominated era. For that, let’s apply the DHOST formalism developed in Ref. [162] in a scenario where the ULDM is non-minimally coupled to gravity. We considering the following action [157, 191]:

$$S = \int d^4x \sqrt{-\tilde{g}} \left[\frac{1}{2} \tilde{R} + \frac{1}{2} \tilde{X} + \frac{1}{2} m \phi^2 - \frac{\lambda}{4} \phi^4 + \tilde{G}^{\mu\nu} \frac{\phi_\mu \phi_\nu}{\Lambda^2} \right] + S_M(\tilde{g}_{\mu\nu}, \psi). \quad (3.1)$$

We work in the so-called GW frame, in which the propagation of GW satisfies the equation of motion of canonical tensor modes given by:

$$v'' + \left(k^2 - \frac{a''}{a}\right)v = 0. \quad (3.2)$$

In GW frame, the modifications of gravity are encoded in the scale factor. It is convenient to rewrite the DHOST theory in the GW frame by considering the following general disformal transformation [162]:

$$\tilde{g}_{\mu\nu} = \left(1 + \hat{D}(\phi, X)X\right) C(\phi, X)g_{\mu\nu}, \quad (3.3)$$

where $C(\phi, X)$ and $\hat{D}(\phi, X)$ are expanded up to $\mathcal{O}(\frac{X}{\Lambda^2})$ as

$$C(X, \phi) \simeq 1 - \frac{6X}{\Lambda^2}, \quad (3.4)$$

$$\hat{D}(X, \phi) \simeq -\frac{2}{\Lambda^2} + \frac{8X}{\Lambda^4}, \quad (3.5)$$

in the perspective of EFT of gravity with a cut-off scale Λ .

Considering the background equation of motion for ϕ up to first order of $\mathcal{O}(\frac{X}{\Lambda^2})$:

$$\ddot{\phi} + 3H\dot{\phi} + m^2\phi + \lambda\phi^3 = \mathcal{O}\left(\frac{X}{\Lambda^2}\right). \quad (3.6)$$

In the regime where the self-interaction term dominates the potential $\lambda\phi^2 \gg m^2$, as expected to happen in the early universe, we obtain:

$$\phi \simeq \frac{\phi_0}{a} \text{sn}(x, -1) \quad , \quad X \simeq \frac{\phi_0^2 \omega^2}{2a^4} \left(\text{cn}(x, -1) \text{dn}(x, -1) - \frac{\mathcal{H}}{\omega} \text{sn}(x, -1) \right)^2, \quad (3.7)$$

where

$$x = \omega(\tau - \tau_*) \quad , \quad \omega = \sqrt{\lambda\phi_0^2/2}. \quad (3.8)$$

In the previous equations, $\text{sn}(x, -1)$, $\text{cn}(x, -1)$ and $\text{dn}(x, -1)$ are the Jacobi elliptic functions, τ_* is the conformal time at the onset of the resonance and ω is the oscillation frequency of the ULDM field when it dominates the potential energy. From now on, we will use the convention $\text{sn}(x, -1) \equiv \text{sn}(x)$, $\text{cn}(x, -1) \equiv \text{cn}(x)$, $\text{dn}(x, -1) \equiv \text{dn}(x)$, for the three functions separately.

When the self-interaction term dominates, this scalar field behaves like radiation. Only when the mass term dominates the potential, it starts to behave like dark matter, which happens for a time $\tau \geq \tau_t$, where τ_t is the transition time, defined through the relation $m^2 a(\tau_t)^2 = \lambda\phi_0^2$. We require this to occur before the radiation-matter equality, $\tau_t < \tau_{eq}$ [162].

For the tensor modes, we will focus on the dominant terms of Eq. (3.7) when $\omega \gg \mathcal{H}$ and $\phi_0 \ll 1$. Expanding the scale factor and its derivative over conformal time in the GW frame, up to the order of $\beta = \mathcal{H}/\omega$, we obtain the following equation for canonical tensor mode variable,

$$\frac{d^2v}{dx^2} + \left[\kappa^2 - 120\alpha^2(\text{sn}^2(x) - 4\text{sn}^6(x) + 4\text{sn}^{10}(x)) \right. \\ \left. + 120\beta\alpha^2\text{cn}(x)\text{sn}^3(x)\text{dn}(x)(8 - 11\text{sn}^4(x)) \right] v \simeq 0, \quad (3.9)$$

where the parameters are defined as:

$$\kappa = \frac{k}{\omega}, \quad \alpha = \frac{\phi_0^2 \omega^2}{a^4 \Lambda^2} \equiv \frac{\alpha_\star}{(1 + \beta_\star x)^4}, \quad \beta = \frac{\mathcal{H}}{\omega} \equiv \frac{\beta_\star}{1 + \beta_\star x}, \quad a(x) = a_\star (1 + \beta_\star x). \quad (3.10)$$

In Eq. (3.10), the terms with a star means that it was evaluated at $\tau = \tau_\star$. The leading term in Eq. (3.9) scales as α_\star , this term controls the strength of the resonance, and corresponds to X^2/Λ^4 . The parameter β_\star determines how long the mode will remain inside the resonance band.

3.1.1 Key Parameters

Now that we have described the formalism, we can study how the parameters affects the resonance, which will be important to describe the results in Sec. 4. First, as stated in Ref. [162], the enhancement is highly sensitive to α_\star , and for it to be significant, we need to require that:

$$\frac{\alpha_\star^4}{\beta_\star} \sim \left(\frac{H_\star}{\Lambda}\right)^8 \left(\frac{a_t}{a_{eq}}\right)^4 \frac{m}{H_\star} \frac{\alpha(\tau_t)}{a_\star} \sim 10^{21} \left(\frac{m}{\text{eV}}\right) \left(\frac{\text{MeV}}{T_\star}\right) \left(\frac{T_{eq}}{T_t}\right)^5 \left(\frac{H_\star}{\Lambda}\right)^8 \gtrsim 1. \quad (3.11)$$

The previous equation provides a lower bound for the mass of the scalar field. We will also require that the EFT approximation holds up to BBN, so the scalar field is frozen before BBN. This way, all the modifications are negligible in the early universe. The scale factor on the onset of the resonance thus is $a_\star < 10^{-8}$, and only after that time, the modifications in the gravity becomes relevant.

The resonance frequency $f \sim \omega$ is related to the mass m or the coupling of the quartic interaction λ via Eq. (3.8) ($\omega \sim m a_t$), which in terms of the model parameter is given by:

$$f \sim \omega \sim 10^{11} \left(\frac{m}{\text{eV}}\right) \left(\frac{a_t}{10^{-4}}\right) \text{ Hz}. \quad (3.12)$$

For the parameters inside LISA band ($f_{\text{LISA}} \sim 10^{-2}$ Hz), we can consider the following relations for the parameters:

$$\begin{aligned} m &\sim 10^{-13} \left(\frac{10^{-4}}{a_t}\right) \text{ eV}, \\ \beta_\star &\sim 10^{-7} \left(\frac{T_\star}{10 \text{ MeV}}\right)^2 \left(\frac{a_\star}{10^{-8}}\right), \\ \frac{\alpha_\star^4}{\beta_\star} &\sim 10^9 \left(\frac{10^{-4}}{a_t}\right) \left(\frac{10 \text{ MeV}}{T_\star}\right) \left(\frac{T_{eq}}{T_t}\right)^5 \left(\frac{H_\star}{\Lambda}\right)^8. \end{aligned}$$

In order to estimate the gravitational wave spectrum nowadays $\Omega_{\text{GW}}(t_0)$, we will consider the amplification occurring on very short timescales in comparison to the Hubble parameter. Afterwards, the tensor modes will evolve like in GR. This way, the amplification can be estimated simply by using the following equation [162]:

$$\Omega_{\text{GW}}(t_0) = \Omega_{\text{GW}}^{\text{Background}}(t_0) \cdot v_p^2, \quad (3.13)$$

where $\Omega_{\text{GW}}^{\text{Background}}(t_0)$ is the spectrum for the background evolution of the universe without considering the resonance, and v_p is the value of the tensor modes after they reach a plateau.

As we have seen in Sec. 2, the background equation for the GW spectrum can have contributions to the tilt from a non standard early universe dynamics, where the spectrum is given during the radiation dominated era by Eq. (2.18).

It is important to note that the resonance will cause a direct amplification on certain narrow frequency bands, as we will see in Sec. 4. The exact effect in the background is given by numerically solving Eq. (3.9).

4 Results and Discussion

In this section, we present the relevant plots and assess the detection prospects for the primordial stochastic gravitational wave background, using the SSR effect to probe the stochastic signal. We consider a primordial spectrum parametrized by different values of the tensor-to-scalar ratio r and the tensor spectral index n_t , as described in Section 2. We consider the spectrum of the modes that re-enter the horizon during the radiation-dominated era. The end of inflation corresponds to higher frequencies, not probed by LISA.

The resonance is obtained by solving Eq. (3.9). To give an example, we will select the resonance parameters to the same values previously provided in [162]: α_* , β_* and ω . For all the plots in this section, we have tuned the value of α_* , which is the parameter that controls the strength of the resonance, to be $\alpha_* = 0.1$. We also set β_* , the parameter that controls how long the modes stay in the resonance band, to the value $\beta_* = 0.0004$ ⁴. Furthermore, we choose $\omega = 10^{-2}\text{Hz}$, so that the resulting resonance peaks fall within the LISA frequency band. This parameter controls when the resonance takes effect, and by changing it, we are able to access when the SSR effect becomes active (by making it higher, we can consider resonances happening in earlier times). The astrophysical foreground, as constructed in Sec. 2.2, is also present in the figures of this section.

In Fig. 2, we plot the spectrum using the value provided by Planck for the tensor-to-scalar ratio ($r = 0.035$). The standard signal generated by slow roll inflation is shown in light gray, and the signal generated by blue tilted model with a non standard value of n_t in gold. The sensitivity curve of LISA is plotted by using the package SGWBProbe, according to the procedure described in Ref. [182].

In the left panel of Fig. 2, we have the background model with highest tensor spectral index ($n_t = 0.22$) that does not produce a detectable signal without the resonance in LISA band. The first peak that already had sufficient amplitude to be detected by LISA is amplified due to the blue tilted background spectrum, which enhance modes at higher frequencies. With this choice of parameter, the other peaks, which would not be detectable in the standard background, are amplified to higher amplitudes, bringing the signal into observable range above all the astrophysical foreground.

In the right panel of Fig. 2, we show the background model with highest value of the tensor spectral index ($n_t = 0.135$) that fully avoids the constraints from BBN. As expected, the amplification is lower in this case, but the resonance effect could still probe the background parameters by the signal obtained by the second peak (still above the astrophysical foreground) and third peak (which, while below the foreground, remains within LISA's detectable range). We have checked that even with a slightly lower value of n_t , a second peak could still be

⁴We tested several other parameter combinations respecting the relations presented in Sec. 3 and found that varying α_* and β_* did not significantly alter the resonance's overall shape. The main results are not very sensitive to that choice.

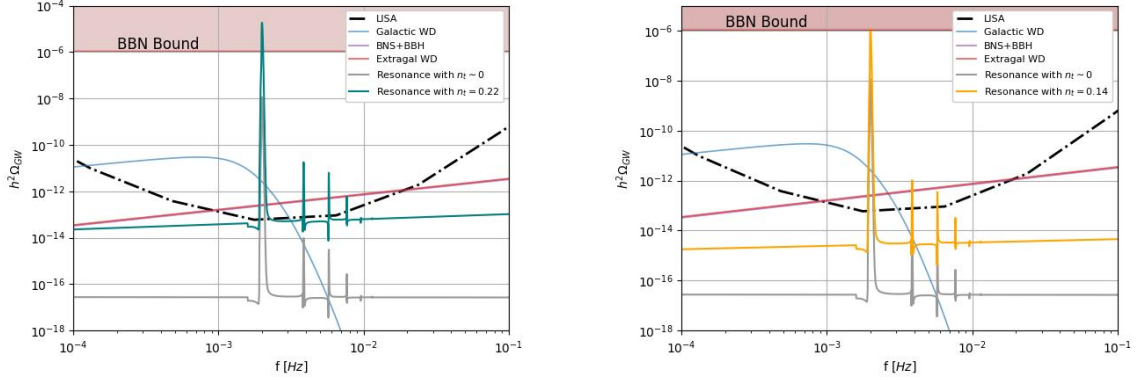


Figure 2: Comparison of the resonant GW spectrum with $r = 0.035$ with the astrophysical foreground generated by the unresolved galactic white dwarf (blue); extragalactic white dwarf (red), the sum of the unresolved contribution to binary neutron star, binary black holes and black hole - neutron star binaries (magenta). In the left panel, the teal curve shows the resonance effect on a blue-tilted background with $n_t = 0.22$. In the right panel, the orange curve represents the resonance on a background with $n_t = 0.135$. The gray curve shows the resonance effect for a standard slow-roll inflationary scenario (where the spectral index follows the inflationary slow-roll consistency relation $n_t \sim 0$). The red shaded region represents the parameter space excluded by the BBN constraint.

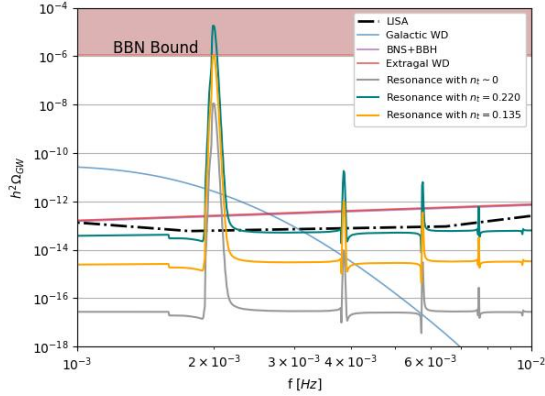


Figure 3: Plot comparing all the three models. In this plot, the background has $r = 0.035$. We show the case with $n_t \sim 0$ in gray, the blue tilted case with $n_t = 0.135$ in orange and $n_t = 0.22$ in teal. The legend is the same as in Figure 2.

detectable inside the LISA band, but the amplitude may be too low to distinguish easily from the astrophysical foreground or the detector noise.

In Fig. 3, we show a close up view of all the three models together with the astrophysical foreground for a more direct visual comparison of the effects generated by the difference in the value of n_t . It is worth emphasizing that all the models considered here are consistent with the upper bounds on the amplitude of the SGWB imposed by LIGO.

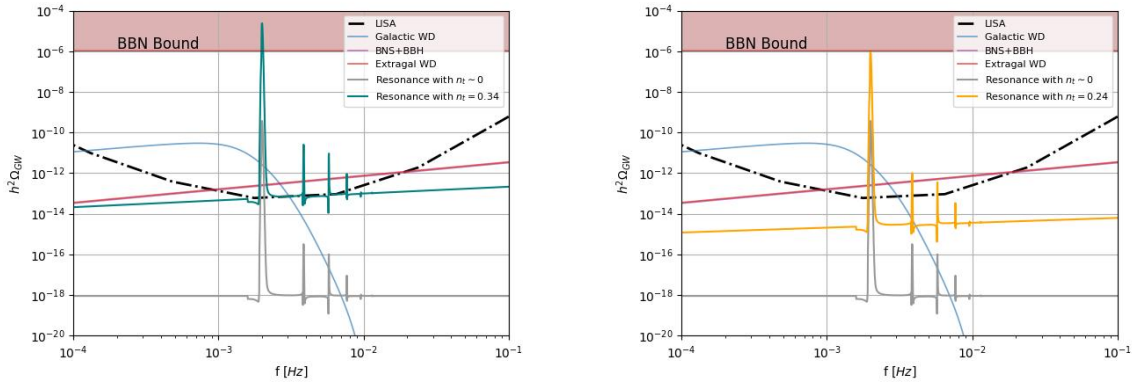


Figure 4: Comparison of GW spectra for the resonance effect with a background parametrized by $r = 1 \cdot 10^{-3}$. The colors are the same as in Fig. 2. In this case, the curve represents the same resonance effect happening in a blue-tilted background with $n_t = 0.336$ (teal) in the left panel and with $n_t = 0.240$ (orange) in the right panel. The red shaded region represents the excluded region by the BBN constraint and the astrophysical foreground is the same as before.

On another note, the resonance effect also allows us to explore what happens to the detection of a background with lower values of the tensor-to-scalar ratio. In the case of $r = 1 \cdot 10^{-3}$, as shown in Fig. 4, we can see that the first peak would still be detectable in the baseline model. But if we compare the resonance to a model with a maximum value of the tensor index $n_t = 0.336$ (or $n_t = 0.240$ to satisfy the limit imposed by the BBN constraint), the second and third peaks would be inside the LISA’s detectable frequency band, similar to the previous case of $r = 0.035$.

4.1 The spectrum of SGWB in the presence of resonance: The role of each parameter

The most promising detection prospects for a blue tilted spectrum happens if the value of r is orders of magnitude lower than the Planck upper bound. For a better visualization of this effect, we plot the results for $r = 10^{-10}$ in Fig. 5, which allows us to explore a higher range of blue tilted spectrum. This figure shows how the signal changes different values of n_t , while it lies in the range $n_t \in [0, 1]$. Changing the value of the spectral index generates a stronger amplification for the smaller peaks as compared to the first one, leading them to a possible observable range for an value of n_t that could be more favorable to blue tilted models that are studied in the literature. Overall, the effect of a lower value of tensor-to-scalar ratio is a considerably reduction of the amplitude of the full spectrum, across every frequency. In that sense, it becomes difficult to determine whether the reduction is due to any alteration in the SSR mechanism (e.g., a reduction of the overall amplitude of the resonance) or simply a lower value of r of the background spectrum by just studying the signal by itself.

Figure 6 shows the effect of the change in r in the theoretical prediction for the spectrum. In this plot, we have fixed the value of the tensor index to be $n_t = 0.5$ and plotted the prediction for the resonant GW spectrum for r to range on four specific values ranging from $r = 10^{-10}$ until $r = 10^{-3}$, comparing with the results for the SSR happening on a background

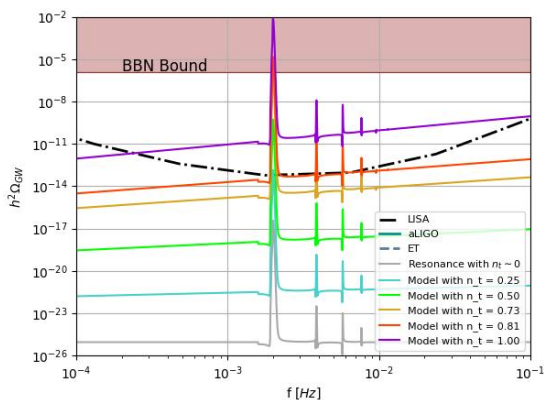


Figure 5: Comparison of different values of tensor spectral index in the range $n_t \in [0, 1]$. In this plot, we consider $r = 10^{-10}$. Specifically, we show the curves where $n_t = 0.73$ (in orange), which would be able to satisfy the BBN bound and the case with $n_t = 0.81$ (in red), which the background signal would be inside LISA’s sensitivity but is ruled out by the BBN constraint. LISA’s sensitivity curve is in black. The light red shaded region represents the region excluded BBN constraints.

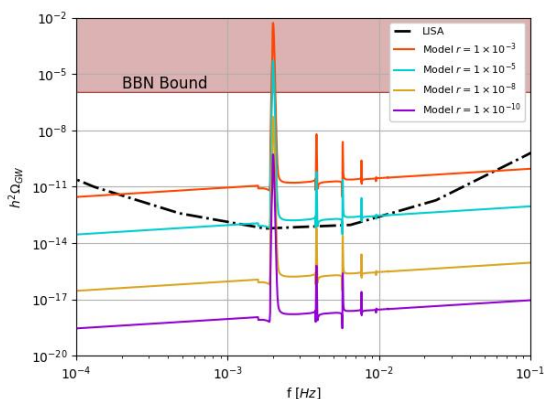


Figure 6: Plot comparing different values of r when $n_t = 0.5$. The blue curve represent the case of $r = 0.035$ with the normal tensor tilt $n_t \sim 0$, while the other curves represents the cases of $r = 10^{-10}$ (magenta), $r = 10^{-8}$ (orange), $r = 10^{-5}$ (blue) and $r = 10^{-3}$ (red). The BBN bound is represented by the red shaded region.

parametrized by the Planck value, $r = 0.035$ and $n_t \sim 0$. As expected, the only effect that the tensor-to-scalar ratio has in the signal is to change the total amplitude of the spectrum. In order for the resonant spectrum to be detectable, a lower value of r requires a correspondingly higher blue tilted spectral index for the primordial background to compensate for the reduced amplitude.

4.2 Probing the primordial spectrum parameters with resonance

As presented in the previous section, one of the interesting features of the resonance effect is the possibility to amplify the cosmological signal in the LISA frequency band. By consider-

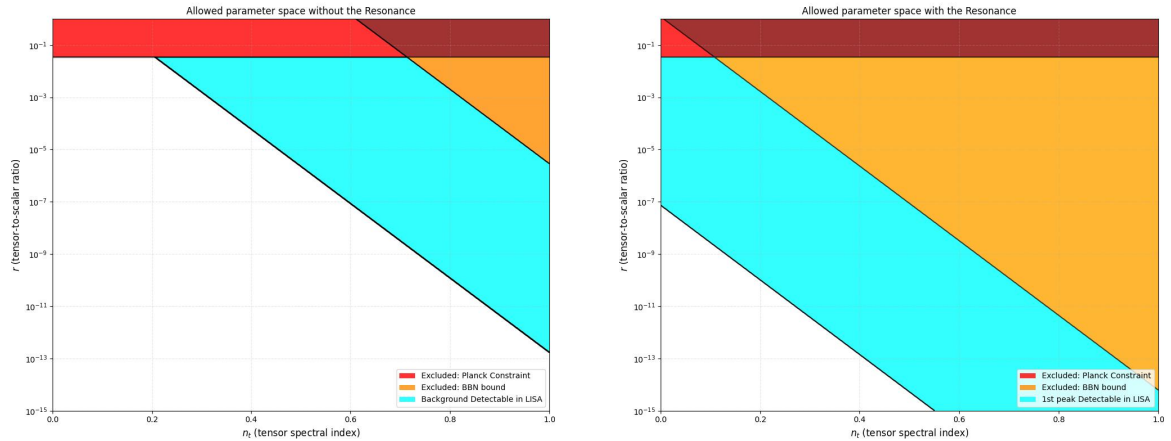


Figure 7: Comparison of the parameter space in the r - n_t plane that would make a detectable signal in LISA (blue region). On the left, we have the constraints in the spectrum without the resonance, and on the right, we have the constraints when the resonance happens. The red region is related to the parameters excluded by Planck, while the orange region represents the parameter subset excluded by the BBN bound.

ing different combinations of the tensor-to-scalar ratio and the spectral index, we find that the resonance can amplify the gravitational-wave background, potentially bringing it within observational reach. Although smaller values of r relax the BBN constraints for a given spectral index, the presence of resonance can lead to a violation of these bounds. It is therefore important to determine how resonance modifies the allowed parameter space.

Considering the minimum frequency at which LISA can detect a signal, $f_{\min} \sim 1.8 \times 10^{-3} \text{Hz}$, we plot in Figure 7 how the resonance affects the possible parameter space accessible to LISA. In the left panel, we show the allowed parameter space for a cosmological background in the absence of the resonance that could generate a detectable signal, in the blue shaded region. The red region represents the Planck upper bound in r and the orange region denotes the part of the parameter space that violates the BBN bound within the LISA frequency range.

On the right panel of Fig. 7, we show the allowed parameter space for a cosmological background in the presence of the resonance studied in this work. As can be seen, the presence of resonance significantly alters the allowed parameter space compared to the case without resonance. The region corresponding to a detectable signal (blue) changes, indicating that the presence of the resonance can amplify a small signal to detectable levels or even exceed the BBN limit for a broader range for the value of the tensor-to-scalar ratio for the background, as shown in Figure 5. On another hand, for a fixed value of r , the presence of resonance allows to probe a wider range of the spectral index, as illustrated in Figure 6. With the resonance included, we observe a shift in the region that violates the BBN constraint when analyzing the first peak, which occurs at a frequency $f_{\text{peak } 1} \sim 2.0 \times 10^{-3} \text{, Hz}$.

In Figure 8, we compare this change in the parameter space visually. The dark blue region is related to the parameter space that generate a detectable signal in LISA with the absence of the resonance, while the light blue is related for the parameter space in the presence of it. As one can see, the region that violates BBN constraint shifts when one consider the

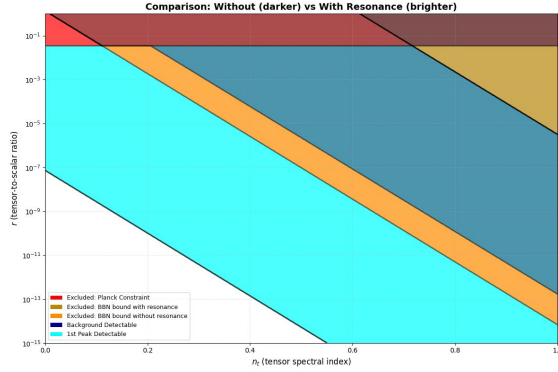


Figure 8: Comparison of the parameter space in the r - n_t plane that could be probed by LISA in the absence (dark blue region) and in the presence (light blue region) of the resonant peaks. The red region is related to the parameters excluded by Planck, while the orange region represents the parameter subset excluded by the BBN bound.

resonance (from the dark orange to the full orange region).

5 Conclusion

It has been shown in the literature that extensions of general relativity involving additional gravitational degrees of freedom, such as scalar fields, can modify the propagation of gravitational waves, leading to the appearance of resonant features in the gravitational wave spectrum. We investigated the prospects for detecting a primordial GW signal in the presence of such resonance. While the ultralight dark matter scenario considered in this paper is only one realization of the parametric resonance effect, our overall qualitative results remains general.

We showed that, in certain scenarios, the resonance can enhance the spectrum to amplitudes within the sensitivity range of the forthcoming detector LISA, leading to a possible detection of one or more features of the resonant amplification. Furthermore, we have demonstrated how the presence of resonance significantly reshapes the region of parameter space accessible to LISA in the r - n_T plane, enabling the experiment to probe lower primordial signals than would be possible in the absence of resonance.

As is well known, within the narrow frequency band probed by a single experiment there are limited prospects for independently constraining the parameters r and n_t , even in the idealized case where a primordial signal is unambiguously detected. The restricted frequency coverage leads to a strong degeneracy between these parameters. To obtain independent constraints on n_t , joint measurements of the spectrum across multiple frequency bands would be required, enabling a multi-frequency test of the gravitational-wave spectrum. Encouragingly, the coming years offer promising prospects for such multi-frequency observations, which could help break the degeneracy in the r - n_t plane. However, for more resonant peaks to be detectable, it would be necessary to have a blue tilted spectrum, which would be a hint for new physics.

Acknowledgments

We are grateful to Manqi Li and Mian Zhu for valuable discussions and comments. This work was supported in part by the National Key R&D Program of China (2021YFC2203100), by NSFC (12433002, W2533006), by CAS young interdisciplinary innovation team (JCTD-2022-20), by 111 Project (B23042), by CSC Innovation Talent Funds, by USTC Fellowship for International Cooperation, and by USTC Research Funds of the Double First-Class Initiative. I.O.C.P. is also supported by ANSO and CAPES. L.G is supported by research grants from Conselho Nacional de Desenvolvimento Científico e Tecnológico (CNPq), Grant No. 307636/2023-2 and from the Fundacao Carlos Chagas Filho de Amparo a Pesquisa do Estado do Rio de Janeiro (FAPERJ), Grant No. E-26/204.598/2024.

References

- [1] B. P. Abbott *et al.* (LIGO Scientific, Virgo), *Phys. Rev. Lett.* **116**, 061102 (2016), [arXiv:1602.03837 \[gr-qc\]](#) .
- [2] G. Agazie *et al.* (NANOGrav), *Astrophys. J. Lett.* **951**, L8 (2023), [arXiv:2306.16213 \[astro-ph.HE\]](#) .
- [3] B. Goncharov *et al.*, *Astrophys. J. Lett.* **917**, L19 (2021), [arXiv:2107.12112 \[astro-ph.HE\]](#) .
- [4] S. Chen *et al.* (EPTA), *Mon. Not. Roy. Astron. Soc.* **508**, 4970 (2021), [arXiv:2110.13184 \[astro-ph.HE\]](#) .
- [5] J. Antoniadis *et al.*, *Mon. Not. Roy. Astron. Soc.* **510**, 4873 (2022), [arXiv:2201.03980 \[astro-ph.HE\]](#) .
- [6] A. Afzal *et al.* (NANOGrav), *Astrophys. J. Lett.* **951**, L11 (2023), [Erratum: *Astrophys.J.Lett.* 971, L27 (2024), Erratum: *Astrophys.J.* 971, L27 (2024)], [arXiv:2306.16219 \[astro-ph.HE\]](#) .
- [7] N. Aghanim *et al.* (Planck), *Astron. Astrophys.* **641**, A6 (2020), [Erratum: *Astron.Astrophys.* 652, C4 (2021)], [arXiv:1807.06209 \[astro-ph.CO\]](#) .
- [8] M. Tristram *et al.*, *Astron. Astrophys.* **647**, A128 (2021), [arXiv:2010.01139 \[astro-ph.CO\]](#) .
- [9] S. Kuroyanagi, T. Takahashi, and S. Yokoyama, *JCAP* **02**, 003 (2015), [arXiv:1407.4785 \[astro-ph.CO\]](#) .
- [10] S. Vagnozzi, *JHEAp* **39**, 81 (2023), [arXiv:2306.16912 \[astro-ph.CO\]](#) .
- [11] S. Kawai and J. Kim, *Phys. Rev. D* **108**, 103537 (2023), [arXiv:2308.13272 \[astro-ph.CO\]](#) .
- [12] Y.-S. Piao and Y.-Z. Zhang, *Phys. Rev. D* **70**, 063513 (2004), [arXiv:astro-ph/0401231](#) .
- [13] T. Kobayashi, M. Yamaguchi, and J. Yokoyama, *Prog. Theor. Phys.* **126**, 511 (2011), [arXiv:1105.5723 \[hep-th\]](#) .
- [14] Y.-F. Cai, J.-O. Gong, and S. Pi, *Phys. Lett. B* **738**, 20 (2014), [arXiv:1404.2560 \[hep-th\]](#) .
- [15] Y.-F. Cai, J.-O. Gong, S. Pi, E. N. Saridakis, and S.-Y. Wu, *Nucl. Phys. B* **900**, 517 (2015), [arXiv:1412.7241 \[hep-th\]](#) .
- [16] D. Cannone, G. Tasinato, and D. Wands, *JCAP* **01**, 029 (2015), [arXiv:1409.6568 \[astro-ph.CO\]](#) .
- [17] B. R. Dinda, S. Kumar, and A. A. Sen, *Phys. Rev. D* **90**, 083515 (2014), [arXiv:1404.3683 \[astro-ph.CO\]](#) .
- [18] Y. Wang and W. Xue, *JCAP* **10**, 075 (2014), [arXiv:1403.5817 \[astro-ph.CO\]](#) .

- [19] S. Choudhury, *Eur. Phys. J. C* **84**, 278 (2024), [arXiv:2307.03249 \[astro-ph.CO\]](#) .
- [20] J.-Q. Jiang, Y. Cai, G. Ye, and Y.-S. Piao, *JCAP* **05**, 004 (2024), [arXiv:2307.15547 \[astro-ph.CO\]](#) .
- [21] M. Chianese, S. Datta, R. Samanta, and N. Saviano, *JCAP* **11**, 051 (2024), [arXiv:2405.00641 \[hep-ph\]](#) .
- [22] I. Ben-Dayan, U. Kumar, U. Thattarampilly, and A. Verma, *Phys. Rev. D* **108**, 103507 (2023), [arXiv:2307.15123 \[astro-ph.CO\]](#) .
- [23] B. Li, J. Meyers, and P. R. Shapiro, *Astrophys. J.* **985**, 117 (2025), [arXiv:2503.18937 \[astro-ph.CO\]](#) .
- [24] N. Barnaby, E. Pajer, and M. Peloso, *Phys. Rev. D* **85**, 023525 (2012), [arXiv:1110.3327 \[astro-ph.CO\]](#) .
- [25] V. Domcke, M. Pieroni, and P. Binétruy, *JCAP* **06**, 031 (2016), [arXiv:1603.01287 \[astro-ph.CO\]](#) .
- [26] D. Jiménez, K. Kamada, K. Schmitz, and X.-J. Xu, *JCAP* **12**, 011 (2017), [arXiv:1707.07943 \[hep-ph\]](#) .
- [27] A. Papageorgiou, M. Peloso, and C. Unal, *JCAP* **07**, 004 (2019), [arXiv:1904.01488 \[astro-ph.CO\]](#) .
- [28] F. D’Eramo and K. Schmitz, *Phys. Rev. Research.* **1**, 013010 (2019), [arXiv:1904.07870 \[hep-ph\]](#) .
- [29] P. Peter, E. J. C. Pinho, and N. Pinto-Neto, *Phys. Rev. D* **73**, 104017 (2006), [arXiv:gr-qc/0605060](#) .
- [30] Y.-F. Cai, D. A. Easson, and R. Brandenberger, *JCAP* **08**, 020 (2012), [arXiv:1206.2382 \[hep-th\]](#) .
- [31] Y.-F. Cai, *Sci. China Phys. Mech. Astron.* **57**, 1414 (2014), [arXiv:1405.1369 \[hep-th\]](#) .
- [32] D. Battefeld and P. Peter, *Phys. Rept.* **571**, 1 (2015), [arXiv:1406.2790 \[astro-ph.CO\]](#) .
- [33] R. Brandenberger and P. Peter, *Found. Phys.* **47**, 797 (2017), [arXiv:1603.05834 \[hep-th\]](#) .
- [34] Y.-F. Cai, A. Marciano, D.-G. Wang, and E. Wilson-Ewing, *Universe* **3**, 1 (2016), [arXiv:1610.00938 \[astro-ph.CO\]](#) .
- [35] S. D. Odintsov, V. K. Oikonomou, F. P. Fronimos, and K. V. Fasoulakos, *Phys. Rev. D* **102**, 104042 (2020), [arXiv:2010.13580 \[gr-qc\]](#) .
- [36] T. Papanikolaou, S. Banerjee, Y.-F. Cai, S. Capozziello, and E. N. Saridakis, *JCAP* **06**, 066 (2024), [arXiv:2404.03779 \[gr-qc\]](#) .
- [37] X.-J. Liu, W. Zhao, Y. Zhang, and Z.-H. Zhu, *Phys. Rev. D* **93**, 024031 (2016), [arXiv:1509.03524 \[astro-ph.CO\]](#) .
- [38] R. R. L. d. Santos and L. M. van Manen, (2022), [arXiv:2212.05594 \[astro-ph.CO\]](#) .
- [39] W. Ahmed, T. A. Chowdhury, S. Nasri, and S. Saad, *Phys. Rev. D* **109**, 015008 (2024), [arXiv:2308.13248 \[hep-ph\]](#) .
- [40] C. Caprini, R. Jinno, M. Lewicki, E. Madge, M. Merchand, G. Nardini, M. Pieroni, A. Roper Pol, and V. Vaskonen (LISA Cosmology Working Group), *JCAP* **10**, 020 (2024), [arXiv:2403.03723 \[astro-ph.CO\]](#) .
- [41] K. Schmitz and T. Schroeder, *JCAP* **01**, 025 (2026), [arXiv:2412.20907 \[astro-ph.CO\]](#) .
- [42] J. L. Cook and L. Sorbo, *Phys. Rev. D* **85**, 023534 (2012), [Erratum: *Phys.Rev.D* 86, 069901 (2012)], [arXiv:1109.0022 \[astro-ph.CO\]](#) .

- [43] S. Mukohyama, R. Namba, M. Peloso, and G. Shiu, *JCAP* **08**, 036 (2014), [arXiv:1405.0346 \[astro-ph.CO\]](#) .
- [44] W. S. Hipolito-Ricaldi, R. Brandenberger, E. G. M. Ferreira, and L. L. Graef, *JCAP* **11**, 024 (2016), [arXiv:1605.04670 \[hep-th\]](#) .
- [45] E. Pajer and M. Peloso, *Class. Quant. Grav.* **30**, 214002 (2013), [arXiv:1305.3557 \[hep-th\]](#) .
- [46] E. Dimastrogiovanni, M. Fasiello, and T. Fujita, *JCAP* **01**, 019 (2017), [arXiv:1608.04216 \[astro-ph.CO\]](#) .
- [47] I. Obata, *JCAP* **06**, 050 (2017), [arXiv:1612.08817 \[astro-ph.CO\]](#) .
- [48] P. Adshead, E. Martinec, E. I. Sfakianakis, and M. Wyman, *JHEP* **12**, 137 (2016), [arXiv:1609.04025 \[hep-th\]](#) .
- [49] L. Iacconi, M. Fasiello, H. Assadullahi, and D. Wands, *JCAP* **12**, 005 (2020), [arXiv:2008.00452 \[astro-ph.CO\]](#) .
- [50] R. von Eckardstein, K. Schmitz, and O. Sobol, *JHEP* **01**, 018 (2026), [arXiv:2508.00798 \[astro-ph.CO\]](#) .
- [51] R. Myrzakulov, L. Sebastiani, and S. Vagnozzi, *Eur. Phys. J. C* **75**, 444 (2015), [arXiv:1504.07984 \[gr-qc\]](#) .
- [52] T. Fujita, S. Kuroyanagi, S. Mizuno, and S. Mukohyama, *Phys. Lett. B* **789**, 215 (2019), [arXiv:1808.02381 \[gr-qc\]](#) .
- [53] S. D. Odintsov and V. K. Oikonomou, *Phys. Rev. D* **99**, 104070 (2019), [arXiv:1905.03496 \[gr-qc\]](#) .
- [54] S. D. Odintsov and V. K. Oikonomou, *Phys. Rev. D* **101**, 044009 (2020), [arXiv:2001.06830 \[gr-qc\]](#) .
- [55] S. Nojiri, S. D. Odintsov, V. K. Oikonomou, and A. A. Popov, *Phys. Dark Univ.* **28**, 100514 (2020), [arXiv:2002.10402 \[gr-qc\]](#) .
- [56] V. K. Oikonomou and E. C. Lymperiadou, *Symmetry* **14**, 1143 (2022), [arXiv:2206.00721 \[gr-qc\]](#) .
- [57] V. K. Oikonomou, *Astropart. Phys.* **144**, 102777 (2023), [arXiv:2209.09781 \[gr-qc\]](#) .
- [58] S. Capozziello, M. Capriolo, and S. Nojiri, *Phys. Lett. B* **850**, 138510 (2024), [arXiv:2401.06424 \[gr-qc\]](#) .
- [59] V. K. Oikonomou, *Phys. Lett. B* **856**, 138890 (2024), [arXiv:2407.12155 \[gr-qc\]](#) .
- [60] S. Capozziello and Q. Gan, *Phys. Lett. B* **872**, 140038 (2026), [arXiv:2507.06094 \[gr-qc\]](#) .
- [61] T. Papanikolaou and S. Capozziello, (2025), [arXiv:2508.03939 \[astro-ph.CO\]](#) .
- [62] T.-C. Li, T. Zhu, W. Zhao, and A. Wang, *JCAP* **07**, 005 (2024), [arXiv:2403.05841 \[gr-qc\]](#) .
- [63] J. Aasi *et al.* (LIGO Scientific), *Class. Quant. Grav.* **32**, 074001 (2015), [arXiv:1411.4547 \[gr-qc\]](#) .
- [64] F. Acernese *et al.* (VIRGO), *Class. Quant. Grav.* **32**, 024001 (2015), [arXiv:1408.3978 \[gr-qc\]](#) .
- [65] T. Akutsu *et al.* (KAGRA), *Nature Astron.* **3**, 35 (2019), [arXiv:1811.08079 \[gr-qc\]](#) .
- [66] M. Punturo *et al.*, *Class. Quant. Grav.* **27**, 194002 (2010).
- [67] S. Hild *et al.*, *Class. Quant. Grav.* **28**, 094013 (2011), [arXiv:1012.0908 \[gr-qc\]](#) .
- [68] A. Abac *et al.* (ET), (2025), [arXiv:2503.12263 \[gr-qc\]](#) .
- [69] P. Amaro-Seoane *et al.* (LISA), (2017), [arXiv:1702.00786 \[astro-ph.IM\]](#) .
- [70] E. Barausse *et al.*, *Gen. Rel. Grav.* **52**, 81 (2020), [arXiv:2001.09793 \[gr-qc\]](#) .

- [71] K. G. Arun *et al.* (LISA), *Living Rev. Rel.* **25**, 4 (2022), [arXiv:2205.01597 \[gr-qc\]](#) .
- [72] M. Braglia *et al.* (LISA Cosmology Working Group), *JCAP* **11**, 032 (2024), [arXiv:2407.04356 \[astro-ph.CO\]](#) .
- [73] G. Agazie *et al.* (NANOGrav), *Astrophys. J. Lett.* **956**, L3 (2023), [arXiv:2306.16221 \[astro-ph.HE\]](#) .
- [74] G. Agazie *et al.* (NANOGrav), *Astrophys. J. Lett.* **951**, L9 (2023), [arXiv:2306.16217 \[astro-ph.HE\]](#) .
- [75] H. Xu *et al.*, *Res. Astron. Astrophys.* **23**, 075024 (2023), [arXiv:2306.16216 \[astro-ph.HE\]](#) .
- [76] J. Antoniadis *et al.* (EPTA, InPTA:), *Astron. Astrophys.* **678**, A50 (2023), [arXiv:2306.16214 \[astro-ph.HE\]](#) .
- [77] J. Antoniadis *et al.* (EPTA), *Astron. Astrophys.* **678**, A48 (2023), [arXiv:2306.16224 \[astro-ph.HE\]](#) .
- [78] J. Antoniadis *et al.* (EPTA, InPTA), *Astron. Astrophys.* **690**, A118 (2024), [arXiv:2306.16226 \[astro-ph.HE\]](#) .
- [79] A. Zic *et al.*, *Publ. Astron. Soc. Austral.* **40**, e049 (2023), [arXiv:2306.16230 \[astro-ph.HE\]](#) .
- [80] D. J. Reardon *et al.*, *Astrophys. J. Lett.* **951**, L6 (2023), [arXiv:2306.16215 \[astro-ph.HE\]](#) .
- [81] A. Weltman *et al.*, *Publ. Astron. Soc. Austral.* **37**, e002 (2020), [arXiv:1810.02680 \[astro-ph.CO\]](#) .
- [82] Y. Akrami *et al.* (Planck), *Astron. Astrophys.* **641**, A10 (2020), [arXiv:1807.06211 \[astro-ph.CO\]](#) .
- [83] M. Tristram *et al.*, *Phys. Rev. D* **105**, 083524 (2022), [arXiv:2112.07961 \[astro-ph.CO\]](#) .
- [84] L. Balkenhol *et al.*, (2025), [arXiv:2512.10613 \[astro-ph.CO\]](#) .
- [85] B. A. Benson *et al.* (SPT-3G), *Proc. SPIE Int. Soc. Opt. Eng.* **9153**, 91531P (2014), [arXiv:1407.2973 \[astro-ph.IM\]](#) .
- [86] L. Balkenhol *et al.* (SPT-3G), *Phys. Rev. D* **108**, 023510 (2023), [arXiv:2212.05642 \[astro-ph.CO\]](#) .
- [87] J. A. Zebrowski *et al.* (SPT-3G), *Phys. Rev. D* **112**, 123520 (2025), [arXiv:2505.02827 \[astro-ph.CO\]](#) .
- [88] E. Camphuis *et al.* (SPT-3G), (2025), [arXiv:2506.20707 \[astro-ph.CO\]](#) .
- [89] M. Hazumi *et al.*, *J. Low Temp. Phys.* **194**, 443 (2019).
- [90] E. Allys *et al.* (LiteBIRD), *PTEP* **2023**, 042F01 (2023), [arXiv:2202.02773 \[astro-ph.IM\]](#) .
- [91] A. Anand (LiteBIRD), *PoS FRAPWS2024*, 015 (2025).
- [92] E. Komatsu, *Nature Rev. Phys.* **4**, 452 (2022), [arXiv:2202.13919 \[astro-ph.CO\]](#) .
- [93] R. Kallosh and A. Linde, *JCAP* **07**, 002 (2013), [arXiv:1306.5220 \[hep-th\]](#) .
- [94] M. Zhu, A. Ilyas, Y. Zheng, Y.-F. Cai, and E. N. Saridakis, *JCAP* **11**, 045 (2021), [arXiv:2108.01339 \[gr-qc\]](#) .
- [95] G. Rodrigues-da Silva, J. Bezerra-Sobrinho, and L. G. Medeiros, *Phys. Rev. D* **105**, 063504 (2022), [arXiv:2110.15502 \[astro-ph.CO\]](#) .
- [96] Y. Shtanov, V. Sahni, and S. S. Mishra, *JCAP* **03**, 023 (2023), [arXiv:2210.01828 \[gr-qc\]](#) .
- [97] E. G. M. Ferreira, E. McDonough, L. Balkenhol, R. Kallosh, L. Knox, and A. Linde, (2025), [arXiv:2507.12459 \[astro-ph.CO\]](#) .
- [98] R. Kallosh and A. Linde, (2025), [arXiv:2512.02969 \[hep-th\]](#) .

- [99] R. H. Cyburt, B. D. Fields, K. A. Olive, and T.-H. Yeh, *Rev. Mod. Phys.* **88**, 015004 (2016), [arXiv:1505.01076 \[astro-ph.CO\]](#) .
- [100] M. Benetti, L. L. Graef, and S. Vagnozzi, *Phys. Rev. D* **105**, 043520 (2022), [arXiv:2111.04758 \[astro-ph.CO\]](#) .
- [101] S. Wang and Z.-C. Zhao, (2025), [10.1088/1674-1137/ae167c](#), [arXiv:2507.06930 \[astro-ph.CO\]](#) .
- [102] C. De Leo, G. Cañas-Herrera, A. Balaudo, M. Martinelli, A. Silvestri, and T. Baker, (2025), [arXiv:2512.19186 \[astro-ph.CO\]](#) .
- [103] A. Balaudo, M. Pantiri, and A. Silvestri, *JCAP* **02**, 023 (2024), [arXiv:2311.17904 \[astro-ph.CO\]](#) .
- [104] A. Maselli, S. Marassi, V. Ferrari, K. Kokkotas, and R. Schneider, *Phys. Rev. Lett.* **117**, 091102 (2016), [arXiv:1606.04996 \[gr-qc\]](#) .
- [105] G. Cognola, E. Elizalde, S. Nojiri, S. D. Odintsov, and S. Zerbini, *Phys. Rev. D* **73**, 084007 (2006), [arXiv:hep-th/0601008](#) .
- [106] D. Langlois and K. Noui, *JCAP* **02**, 034 (2016), [arXiv:1510.06930 \[gr-qc\]](#) .
- [107] N. Drepanou, A. Lymperis, E. N. Saridakis, and K. Yesmakhanova, *Eur. Phys. J. C* **82**, 449 (2022), [arXiv:2109.09181 \[gr-qc\]](#) .
- [108] P. Brax, S. Casas, H. Desmond, and B. Elder, *Universe* **8**, 11 (2021), [arXiv:2201.10817 \[gr-qc\]](#) .
- [109] V. K. Oikonomou and I. Giannakoudi, *Int. J. Mod. Phys. D* **31**, 2250075 (2022), [arXiv:2205.08599 \[gr-qc\]](#) .
- [110] O. Trivedi, A. Bidlan, and P. Moniz, *Phys. Lett. B* **858**, 139074 (2024), [arXiv:2407.16685 \[gr-qc\]](#) .
- [111] W. Lin, L. Visinelli, and T. T. Yanagida, *JCAP* **10**, 023 (2025), [arXiv:2504.17638 \[astro-ph.CO\]](#) .
- [112] F. Feleppa, G. Lambiase, and S. Vagnozzi, *Phys. Rev. D* **112**, 084011 (2025), [arXiv:2508.18448 \[gr-qc\]](#) .
- [113] D. G. Boulware and S. Deser, *Phys. Rev. Lett.* **55**, 2656 (1985).
- [114] R. Ferraro and F. Fiorini, *Phys. Rev. D* **75**, 084031 (2007), [arXiv:gr-qc/0610067](#) .
- [115] R. Mandal, C. Sarkar, and A. K. Sanyal, *JHEP* **05**, 078 (2018), [arXiv:1801.04056 \[hep-th\]](#) .
- [116] X. Zhang, C.-Y. Chen, and Y. Reyimuaji, *Phys. Rev. D* **105**, 043514 (2022), [arXiv:2108.07546 \[gr-qc\]](#) .
- [117] P. Mocz *et al.*, *Phys. Rev. Lett.* **123**, 141301 (2019), [arXiv:1910.01653 \[astro-ph.GA\]](#) .
- [118] L. Hui, *Ann. Rev. Astron. Astrophys.* **59**, 247 (2021), [arXiv:2101.11735 \[astro-ph.CO\]](#) .
- [119] G. Choi, W. Lin, L. Visinelli, and T. T. Yanagida, *Phys. Rev. D* **104**, L101302 (2021), [arXiv:2106.12602 \[hep-ph\]](#) .
- [120] Y.-D. Tsai, D. Farnocchia, M. Micheli, S. Vagnozzi, and L. Visinelli, *Commun. Phys.* **7**, 311 (2024), [arXiv:2309.13106 \[hep-ph\]](#) .
- [121] M. C. Guzzetti, N. Bartolo, M. Liguori, and S. Matarrese, *Riv. Nuovo Cim.* **39**, 399 (2016), [arXiv:1605.01615 \[astro-ph.CO\]](#) .
- [122] Y.-F. Cai, J. Jiang, M. Sasaki, V. Vardanyan, and Z. Zhou, *Phys. Rev. Lett.* **127**, 251301 (2021), [arXiv:2105.12554 \[astro-ph.CO\]](#) .
- [123] G. Domènech and A. Ganz, *JCAP* **01**, 020 (2025), [arXiv:2406.19950 \[gr-qc\]](#) .

- [124] Y.-F. Cai, X. Tong, D.-G. Wang, and S.-F. Yan, *Phys. Rev. Lett.* **121**, 081306 (2018), [arXiv:1805.03639 \[astro-ph.CO\]](#) .
- [125] Y.-F. Cai, C. Chen, X. Tong, D.-G. Wang, and S.-F. Yan, *Phys. Rev. D* **100**, 043518 (2019), [arXiv:1902.08187 \[astro-ph.CO\]](#) .
- [126] C. Chen and Y.-F. Cai, *JCAP* **10**, 068 (2019), [arXiv:1908.03942 \[astro-ph.CO\]](#) .
- [127] C. Chen, X.-H. Ma, and Y.-F. Cai, *Phys. Rev. D* **102**, 063526 (2020), [arXiv:2003.03821 \[astro-ph.CO\]](#) .
- [128] A. Addazi, S. Capozziello, and Q. Gan, *JCAP* **08**, 051 (2022), [arXiv:2204.07668 \[astro-ph.CO\]](#) .
- [129] J.-H. Jin, Z.-C. Chen, Z. Yi, Z.-Q. You, L. Liu, and Y. Wu, *JCAP* **09**, 016 (2023), [arXiv:2307.08687 \[astro-ph.CO\]](#) .
- [130] Y. Wu, Z.-C. Chen, and L. Liu, *JCAP* **02**, 074 (2025), [arXiv:2409.14929 \[astro-ph.CO\]](#) .
- [131] W. Hu, R. Barkana, and A. Gruzinov, *Phys. Rev. Lett.* **85**, 1158 (2000), [arXiv:astro-ph/0003365](#) .
- [132] A. Arvanitaki, J. Huang, and K. Van Tilburg, *Phys. Rev. D* **91**, 015015 (2015), [arXiv:1405.2925 \[hep-ph\]](#) .
- [133] D. J. E. Marsh, *Phys. Rept.* **643**, 1 (2016), [arXiv:1510.07633 \[astro-ph.CO\]](#) .
- [134] A. Laguë, B. Schwabe, R. Hložek, D. J. E. Marsh, and K. K. Rogers, *Phys. Rev. D* **109**, 043507 (2024), [arXiv:2310.20000 \[astro-ph.CO\]](#) .
- [135] A. E. Nelson and J. Scholtz, *Phys. Rev. D* **84**, 103501 (2011), [arXiv:1105.2812 \[hep-ph\]](#) .
- [136] P. Arias, D. Cadamuro, M. Goodsell, J. Jaeckel, J. Redondo, and A. Ringwald, *JCAP* **06**, 013 (2012), [arXiv:1201.5902 \[hep-ph\]](#) .
- [137] J. Jaeckel and S. Schenk, *Phys. Rev. D* **103**, 103523 (2021), [arXiv:2102.08394 \[hep-ph\]](#) .
- [138] N. Brahma, E. Iles, H. Schéerer, and K. Schutz, (2025), [arXiv:2509.07085 \[hep-ph\]](#) .
- [139] P. Svrcek and E. Witten, *JHEP* **06**, 051 (2006), [arXiv:hep-th/0605206](#) .
- [140] A. Arvanitaki, S. Dimopoulos, S. Dubovsky, N. Kaloper, and J. March-Russell, *Phys. Rev. D* **81**, 123530 (2010), [arXiv:0905.4720 \[hep-th\]](#) .
- [141] M. Cicoli, M. Goodsell, and A. Ringwald, *JHEP* **10**, 146 (2012), [arXiv:1206.0819 \[hep-th\]](#) .
- [142] H. An, F. P. Huang, J. Liu, and W. Xue, *Phys. Rev. Lett.* **126**, 181102 (2021), [arXiv:2010.15836 \[hep-ph\]](#) .
- [143] A. Laguë, J. R. Bond, R. Hložek, K. K. Rogers, D. J. E. Marsh, and D. Grin, *JCAP* **01**, 049 (2022), [arXiv:2104.07802 \[astro-ph.CO\]](#) .
- [144] E. Sheridan, F. Carta, N. Gendler, M. Jain, D. J. E. Marsh, L. McAllister, N. Righi, K. K. Rogers, and A. Schachner, *JHEP* **09**, 016 (2025), [arXiv:2412.12012 \[hep-th\]](#) .
- [145] C. Capanelli, E. G. M. Ferreira, and E. McDonough, (2025), [arXiv:2509.15299 \[astro-ph.CO\]](#) .
- [146] L. Hui, J. P. Ostriker, S. Tremaine, and E. Witten, *Phys. Rev. D* **95**, 043541 (2017), [arXiv:1610.08297 \[astro-ph.CO\]](#) .
- [147] E. G. M. Ferreira, *Astron. Astrophys. Rev.* **29**, 7 (2021), [arXiv:2005.03254 \[astro-ph.CO\]](#) .
- [148] P. C. M. Delgado, *Phys. Rev. D* **108**, 123539 (2023), [arXiv:2309.09946 \[hep-ph\]](#) .
- [149] T. Matos, L. A. Ureña-López, and J.-W. Lee, *Front. Astron. Space Sci.* **11**, 1347518 (2024), [arXiv:2312.00254 \[astro-ph.CO\]](#) .

- [150] S. Lu, A. Ilyas, X.-H. Ma, B. Wang, D. Zhang, and Y.-F. Cai, *JCAP* **01**, 086 (2025), [arXiv:2407.19521 \[astro-ph.CO\]](#) .
- [151] C. A. J. O’Hare, *PoS COSMICWISPers*, 040 (2024), [arXiv:2403.17697 \[hep-ph\]](#) .
- [152] A. Eberhardt and E. G. M. Ferreira, (2025), [arXiv:2507.00705 \[astro-ph.CO\]](#) .
- [153] Q. Yang, B. Li, and P. R. Shapiro, *Sci. China Phys. Mech. Astron.* **68**, 280409 (2025), [arXiv:2503.16773 \[astro-ph.CO\]](#) .
- [154] D. Langlois and K. Noui, *JCAP* **07**, 016 (2016), [arXiv:1512.06820 \[gr-qc\]](#) .
- [155] M. Crisostomi, K. Koyama, and G. Tasinato, *JCAP* **04**, 044 (2016), [arXiv:1602.03119 \[hep-th\]](#) .
- [156] J. Ben Achour, D. Langlois, and K. Noui, *Phys. Rev. D* **93**, 124005 (2016), [arXiv:1602.08398 \[gr-qc\]](#) .
- [157] T. Kobayashi, *Rept. Prog. Phys.* **82**, 086901 (2019), [arXiv:1901.07183 \[gr-qc\]](#) .
- [158] R. P. Woodard, *Lect. Notes Phys.* **720**, 403 (2007), [arXiv:astro-ph/0601672](#) .
- [159] R. P. Woodard, *Scholarpedia* **10**, 32243 (2015), [arXiv:1506.02210 \[hep-th\]](#) .
- [160] V. Pettorino and L. Amendola, *Phys. Lett. B* **742**, 353 (2015), [arXiv:1408.2224 \[astro-ph.CO\]](#) .
- [161] L. Xu, *Phys. Rev. D* **91**, 103520 (2015), [arXiv:1410.6977 \[astro-ph.CO\]](#) .
- [162] Y.-F. Cai, G. Domènech, A. Ganz, J. Jiang, C. Lin, and B. Wang, *JCAP* **10**, 027 (2024), [arXiv:2311.18546 \[gr-qc\]](#) .
- [163] J. D. Bekenstein, *Phys. Rev. D* **48**, 3641 (1993), [arXiv:gr-qc/9211017](#) .
- [164] P. Creminelli, J. Gleyzes, J. Noreña, and F. Vernizzi, *Phys. Rev. Lett.* **113**, 231301 (2014), [arXiv:1407.8439 \[astro-ph.CO\]](#) .
- [165] J. Gleyzes, D. Langlois, F. Piazza, and F. Vernizzi, *JCAP* **02**, 018 (2015), [arXiv:1408.1952 \[astro-ph.CO\]](#) .
- [166] A. Ilyas, M. Zhu, Y. Zheng, Y.-F. Cai, and E. N. Saridakis, *JCAP* **09**, 002 (2020), [arXiv:2002.08269 \[gr-qc\]](#) .
- [167] C. Caprini and D. G. Figueroa, *Class. Quant. Grav.* **35**, 163001 (2018), [arXiv:1801.04268 \[astro-ph.CO\]](#) .
- [168] E. Watanabe, Yuki ; Komatsu, *Phys. Rev. D* **73**, 123515 (2006), [arXiv:astro-ph/0604176](#) .
- [169] P. A. R. Ade *et al.* (Planck), *Astron. Astrophys.* **594**, A13 (2016), [arXiv:1502.01589 \[astro-ph.CO\]](#) .
- [170] T. Kobayashi, M. Yamaguchi, and J. Yokoyama, *Phys. Rev. Lett.* **105**, 231302 (2010), [arXiv:1008.0603 \[hep-th\]](#) .
- [171] J. Martin and R. H. Brandenberger, *Phys. Rev. D* **63**, 123501 (2001), [arXiv:hep-th/0005209](#) .
- [172] A. Bedroya and C. Vafa, *JHEP* **09**, 123 (2020), [arXiv:1909.11063 \[hep-th\]](#) .
- [173] A. Bedroya, R. Brandenberger, M. Loverde, and C. Vafa, *Phys. Rev. D* **101**, 103502 (2020), [arXiv:1909.11106 \[hep-th\]](#) .
- [174] S. Mohanty and A. Nautiyal, (2014), [arXiv:1404.2222 \[hep-ph\]](#) .
- [175] M. Maggiore, *Phys. Rept.* **331**, 283 (2000), [arXiv:gr-qc/9909001](#) .
- [176] A. K. Soman, S. S. Mishra, M. Shafi, and S. Basak, *Phys. Rev. D* **112**, 103521 (2025), [arXiv:2407.07956 \[gr-qc\]](#) .
- [177] S. Saikawa, Ken’ichi ; Shirai, *JCAP* **05**, 035 (2018), [arXiv:1803.01038 \[hep-ph\]](#) .

- [178] S. Kuroyanagi, T. Chiba, and N. Sugiyama, *Phys. Rev. D* **79**, 103501 (2009), [arXiv:0804.3249 \[astro-ph\]](#) .
- [179] S. S. Mishra, V. Sahni, and A. A. Starobinsky, *JCAP* **05**, 075 (2021), [arXiv:2101.00271 \[gr-qc\]](#) .
- [180] T. Kite, J. Chluba, A. Ravenni, and S. P. Patil, *Mon. Not. Roy. Astron. Soc.* **509**, 1366 (2021), [arXiv:2107.13351 \[astro-ph.CO\]](#) .
- [181] B. Allen, in *Les Houches School of Physics: Astrophysical Sources of Gravitational Radiation* (1996) pp. 373–417, [arXiv:gr-qc/9604033](#) .
- [182] P. Campeti, E. Komatsu, D. Poletti, and C. Baccigalupi, *JCAP* **01**, 012 (2021), [arXiv:2007.04241 \[astro-ph.CO\]](#) .
- [183] C. J. Moore, R. H. Cole, and C. P. L. Berry, *Class. Quant. Grav.* **32**, 015014 (2015), [arXiv:1408.0740 \[gr-qc\]](#) .
- [184] C. M. F. Mingarelli, S. R. Taylor, B. S. Sathyaprakash, and W. M. Farr, (2019), [arXiv:1911.09745 \[gr-qc\]](#) .
- [185] N. Cornish and T. Robson, *J. Phys. Conf. Ser.* **840**, 012024 (2017), [arXiv:1703.09858 \[astro-ph.IM\]](#) .
- [186] T. Robson, N. J. Cornish, and C. Liu, *Class. Quant. Grav.* **36**, 105011 (2019), [arXiv:1803.01944 \[astro-ph.HE\]](#) .
- [187] A. Nishizawa, K. Yagi, A. Taruya, and T. Tanaka, *Phys. Rev. D* **85**, 044047 (2012), [arXiv:1110.2865 \[astro-ph.CO\]](#) .
- [188] A. G. Abac *et al.* (LIGO Scientific, VIRGO, KAGRA), (2025), [arXiv:2508.20721 \[gr-qc\]](#) .
- [189] S. Kuroyanagi, T. Takahashi, and S. Yokoyama, *JCAP* **01**, 071 (2021), [arXiv:2011.03323 \[astro-ph.CO\]](#) .
- [190] E. Di Valentino *et al.* (CosmoVerse Network), *Phys. Dark Univ.* **49**, 101965 (2025), [arXiv:2504.01669 \[astro-ph.CO\]](#) .
- [191] G. Gandolfi, B. S. Haridasu, S. Liberati, and A. Lapi, *Astrophys. J.* **952**, 105 (2023), [arXiv:2305.13974 \[astro-ph.CO\]](#) .